Stem Cell Research (2012) 8, 357–367

Available online at www.sciencedirect.com

SciVerse ScienceDirect

www.elsevier.com/locate/scr


# Protective effect of apelin on cultured rat bone marrow mesenchymal stem cells against apoptosis

Xiangjun Zeng [a,b,c], Shan Ping Yu [a], Tammi Taylor [a], Molly Ogle [a,c], Ling Wei [a,c,*]

[a] Department of Anesthesiology, Emory University School of Medicine, Atlanta, GA 30322, USA
[b] Department of Pathophysiology, Capital Medical University, Beijing 100069, China
[c] Department of Pathology, Medical University of South Carolina, Charleston, SC 29425, USA

Received 15 September 2010; received in revised form 23 November 2011; accepted 5 December 2011
Available online 13 December 2011

**Abstract** Bone marrow-derived mesenchymal stem cells (BMSCs) have shown great promise for ischemic tissue repair. However, poor viability of transplanted BMSCs within ischemic tissues has limited their therapeutic potential. Apelin, an endogenous peptide, whose level is elevated following ischemia, has been shown to enhance survival of cardiomyocytes and neuronal cells during ischemia. We hypothesized that apelin-13 protects BMSCs from apoptotic death. In this paper we determined the potential mechanism of apelin-13 effects using cultured BMSCs from adult rats. Apoptosis was induced by the specific apoptotic insult serum deprivation (SD) for up to 36 h. Apoptotic cell death was measured using immunostaining and Western blotting in the presence and absence of apelin-13 (0.1 to 5.0 nM) co-applied during SD exposure. SD-induced apoptosis was significantly reduced by apelin-13 in a concentration-dependent manner. SD-induced mitochondrial depolarization, cytochrome c release, and caspase-3 activation were largely prevented by apelin-13. The apelin-13 anti-apoptotic effects were blocked by inhibiting the MAPK/ERK1/2 and PI3K/Akt signaling pathways. Taken together, our findings indicate that apelin-13 is a survival factor for BMSCs and its anti-apoptotic property may prove to be of therapeutic significance in terms of exploiting BMSC-based transplantation therapy.


## Introduction

Bone marrow-derived mesenchymal stem cells (BMSCs) are self-renewing progenitor cells that differentiate into osteoblasts, chondrocytes, astrocytes, neurons, skeletal muscle cells, and cardiomyocytes in vitro and in vivo (Pereira et al., 1995; Azizi et al., 1998). Besides their differentiating potentials, autologous BMSCs can be isolated from bone marrow and expanded, which makes BMSCs a conceivable source of stem cells for repairing damaged tissues. So far, BMSCs have been tested in several animal brain and heart ischemia models and have shown beneficial effects by promoting tissue repair and functional recovery (Li et al., 2001; Zubko and Frishman, 2009; Hu et al., 2008; Barry and Murphy, 2004). Previous reports have shown that transplanted stem cells including BMSCs do not survive well within diseased tissues (Geng, 2003). For instance, after injection into the left ventricle of immunodeficient adult CB17 SCID/beige mice that are deficient in B- and T-cells, more than 99% of injected

* Corresponding author at: 101 Woodruff Circle, Department of Anesthesiology, Emory University School of Medicine, Atlanta, GA 30322, USA.
*E-mail address:* lwei7@emory.edu (L. Wei).

1873-5061/$ - see front matter © 2012 Elsevier B.V. All rights reserved.
doi:10.1016/j.scr.2011.12.004

cells die within 4 days of injection (Toma et al., 2002). This result provides a piece of compelling evidence that transplanted BMSCs are unlikely eliminated by cells in the immune system, but die due to other mechanisms. Evidence suggests that transplanted cells die from apoptosis (Geng, 2003; Zhang et al., 2001), therefore strategies that enhance tolerance to apoptotic insults should have significant impacts on improving the efficiency of BMSC transplantation therapy.

Apelin is a natural ligand for an orphan G protein coupled receptor, APJ (putative receptor protein related to the angiotensin receptor AT1) (O'Dowd et al., 1993), which had previously been identified by the Human Genome Project in 1993 (O'Dowd et al., 1993; Falcao-Pires and Leite-Moreira, 2005). Apelin is derived from a 77 amino acid length preproapelin that can be cleaved into active apelin containing 13, 17 or 36 amino acids by angiotensin-converting enzymes. The 13C-terminal amino acids are completely conserved across all species (Lee et al., 2000). Moreover, apelin-13 invariably exhibits greater degrees of biological potency (Simpkin et al., 2007). The apelin/APJ system distributes over many tissues, suggesting that they might play broad roles in physiology and pathophysiology. Current data shows that apelin is involved in the regulation of cardiovascular, gastrointestinal, and immune functions, as well as in bone physiology, fluid homeostasis, and cardiovascular system development (Kleinz and Davenport, 2005; Masri et al., 2005). Apelin has been shown to suppress apoptosis in osteoblastic cell line MC3T3-E1 and human osteoblasts via the APJ/PI3K/Akt signaling pathway (Xie et al., 2000; Tang et al., 2007). However, there has been no report about the effect of apelin on the viability of BMSCs.

Serum deprivation (SD) has been widely used as a typical apoptotic insult to a variety of cell types and is regarded as an insult that mimics a major ischemic component *in vivo* (Behrens et al., 1996; Tsubokawa et al., 2010; Chauvier et al., 2005). SD has been shown to induce apoptosis in BMSCs through the mitochondrial pathway (Tatemoto et al., 1998). The present investigation employed this apoptotic model to test the protective effect of apelin-13 on BMSCs. Reactive oxygen species (ROS) generation, mitochondrial depolarization, cytochrome c release, and caspase activation play important roles in the SD-induced neuronal apoptosis (Chauvier et al., 2005). Inhibited PI3K and increased extracellular signal-regulated MAPK (extracellular regulated kinases, ERK1/2) have been linked to SD-induced neuronal apoptosis (Chang et al., 2004). Our recent work shows that apelin-13 is protective against SD- and ischemia-induced cell death in cortical neurons and cardiomyocytes via the mechanism of regulating the ERK1/2 and Akt phosphorylation (Zeng et al., 2009, 2010). Apelin-13 treatment prevented the loss of mitochondrial membrane potential during SD treatment. Moreover, apelin-13 reduced the ROS generation and the cytochrome c release from mitochondria to cytoplasm as well as activation of caspase-3. These results indicate that apelin protects cells via multiple mechanisms (Zeng et al., 2009, 2010). Whether apelin-13 has similar protective effects on undifferentiated stem cells or progenitor cells has not been explored. The present investigation tested the hypothesis that apelin-13 could protect BMSCs from apoptosis by mitochondrial protection mediated by MAPK/ERK1/2 and PI3K/Akt signaling pathways. Data from this investigation may be useful for promoting survival of transplanted BMSCs in ischemic tissue, which will enhance the efficacy of cell therapy.

## Results

### Expression of APJ receptor in BMSCs

Prior to exploring the protective effects of apelin-13 in rat BMSCs, we performed RT-PCR, immunostaining, and Western blotting to examine the mRNA and protein levels of APJ in rat BMSCs. RT-PCR detected expression of APJ mRNA in BMSCs, with confirmation of primer specificity indicated by the signal in PcDNA3.1+/APJ HEK293 cells but not in control HEK293 cells (Fig. 1a). Expression of APJ in rat BMSCs was detected using Immunofluorescence CD90 and APJ staining in BMSCs (Fig. 1b). APJ was confirmed by Western blot analysis (Fig. 1c). APJ expression was not changed by serum deprivation and apelin-13 treatment (Fig. 1c).

### Effect of apelin-13 on BMSC viability

Previously, whether apelin-13 was toxic to BMSCs had not been addressed. We examined the active form of apelin, apelin-13, for its effect on BMSC viability. Trypan blue assay indicated that apelin-13 up to 5 nM had no adverse effect on the viability of BMSCs (Fig. 2a). This is a concentration range with which apelin-13 show neuroprotective effect in cortical neurons (Zeng et al., 2010).

### Apelin-13 protected BMSCs from SD-Induced Apoptosis

Hoechst 33342 and trypan blue staining was applied to detect the SD-induced morphological changes and apoptosis in rat BMSCs. BMSCs were exposed to serum free medium with increasing concentrations of apelin-13 (0.1 to 5 nM) for 36 h. This concentration range was selected based on our previous work on the protective effect of apelin-13 on cortical cultures (Zeng et al., 2010). After SD treatment, cell shrinkage and nuclear condensation were obvious and some cells were fragmented (Fig. 2b). Injured cells failed to exclude trypan blue out, so they became trypan blue positive. SD caused about 50% cell death in trypan blue assay. Co-applied apelin-13 showed a concentration-dependent effect of reducing SD-induced cell death. Apelin-13 at 0.5 and 5 nM significantly attenuated the number of trypan blue positive cells (Fig. 2c). Since the cell death assay was taking place for several hours, we measured cell proliferation activity that might interfere with the cell death assay. In the presence of 5 nM apelin-13 and proliferation marker BrdU, proliferative activity of BrdU-positive BMSCs did not show significant changes during 24-h apelin-13 treatment (Figs. 2e and f).

To further evaluate the effect of apelin-13 on cell death, TUNEL staining was used to detect DNA fragmentation and cell death in SD-treated BMSCs with and without apelin-13 treatment. The 36-h SD insult induced 60% cell death among BMSCs, co-applied apelin-13 (5 nM) significantly increased the survival of BMSCs under the SD condition; about 40% cell death was blocked by the apelin-13 treatment (Fig. 2d). In a

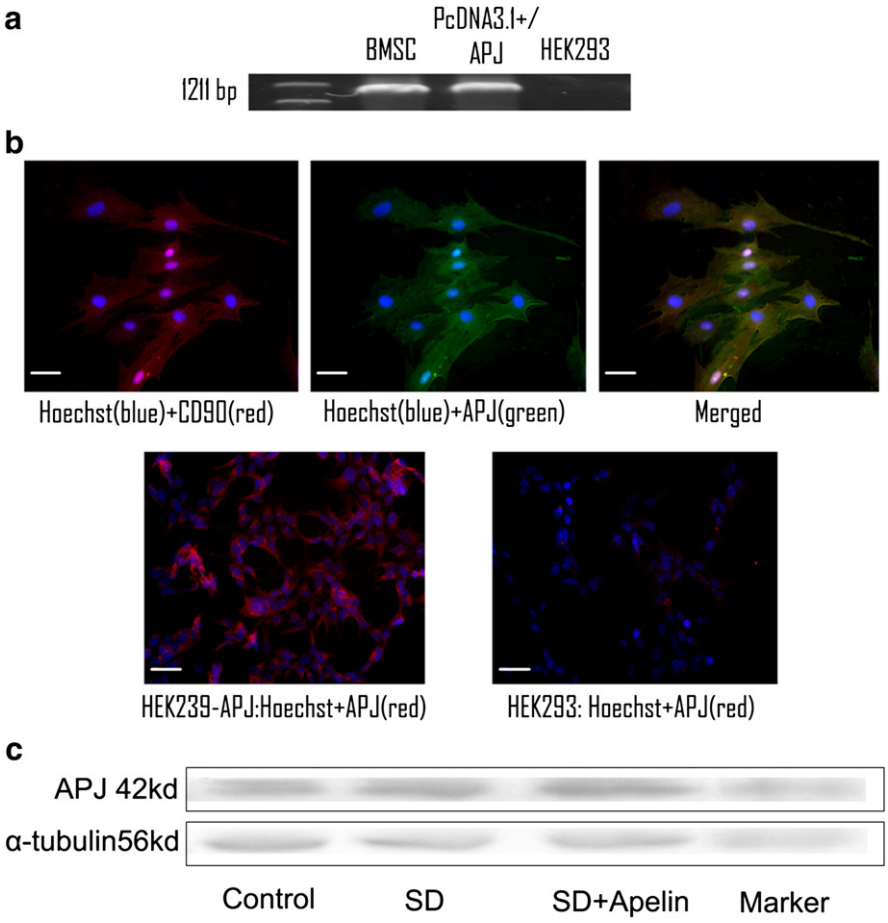


**Figure 1** *Expression of APJ receptor in rat BMSCs.* RT-PCR, immunohistochemistry and Western blotting was applied to confirm expression of the apelin receptor APJ in rat BMSCs. a. RT-PCR detected mRNA expression of APJ in rat BMSCs. APJ primer specificity was verified by RT-PCR detection of APJ mRNA expression in human HEK293 cells as a negative control and a rat APJ-expression plasmid (pcDNA3.1+/APJ) used as a positive PCR control. b. Detection of APJ protein expression in rat BMSCs with an anti-APJ polyclonal antibody and immunoimaging. BMSCs were co-labeled with a PE-conjugated anti-rat CD90 antibody (red), and Hoechst 33342 nuclear label (blue) for total cells. Antibody reactivity was verified by detection of APJ (green) expression in stably transfected HEK293 cells (HEK293-APJ) but not in wild-type HEK293 cells. Scale bar = 50 μm. c. Western blot analysis showed APJ expression in BMSCs. The APJ level was not affected by treatment with serum deprivation (SD) or SD plus apelin-13 (5 nM). All experiments were repeated at least 3 times.

cell death assay of oxygen-glucose deprivation (OGD), apelin-13 did not show significant protection in MTT assays although a trend of reducing OGD-induced cell death was seen. For example, cell survival rate was 26.6% and 18.7% after 24-h OGD with and without co-applied 5 nM apelin-13 ($n=3$, $P=0.07$).

## Protective effect of apelin on mitochondria

TMRM is a lipophilic potentiometric dye which partitions between the mitochondria and cytosol in proportion to mitochondrial membrane potential ($\Delta\psi_m$) by virtue of its positive charge. At low concentrations, the fluorescent intensity is a simple function of dye concentration, which is in turn a direct function of mitochondrial potential and associated mitochondria function. After 12 h in SD TMRM fluorescence was reduced in BMSCs, indicating a depolarization of the mitochondrial membrane. Apelin-13 (0.1–5 nM) prevented the SD-induced decreases in the TMRM fluorescent intensity in a concentration-dependent manner (Fig. 3).

Mitochondrial dysfunction provokes release of cytochrome c from the mitochondria into the cytosol. Western blot analysis revealed that exposure of BMSCs to SD induced a significant increase in cytosolic cytochrome c levels, accompanied by a parallel decrease of cytochrome c in the mitochondrial fraction (Figs. 4a and b). Apelin-13 (0.1–5 nM) treatment concentration-dependently inhibited the cytochrome c release from mitochondria (Figs. 4a and b).

Cytochrome c release leads to activation of caspase-3, which is a key and executing step in the apoptosis process. Western blotting showed that exposure to SD significantly increased caspase-3 activation compared to the enzyme level in control cells (Fig. 4c). Apelin-13 markedly inhibited SD-induced activation of caspase-3, keeping the activity of this enzyme near the control level (Fig. 4c).

## Inhibitory effect of apelin-13 on ROS production

Dihydroethidium (DHE) is the chemically reduced form of the DNA dye ethidium bromide. This probe is widely used in

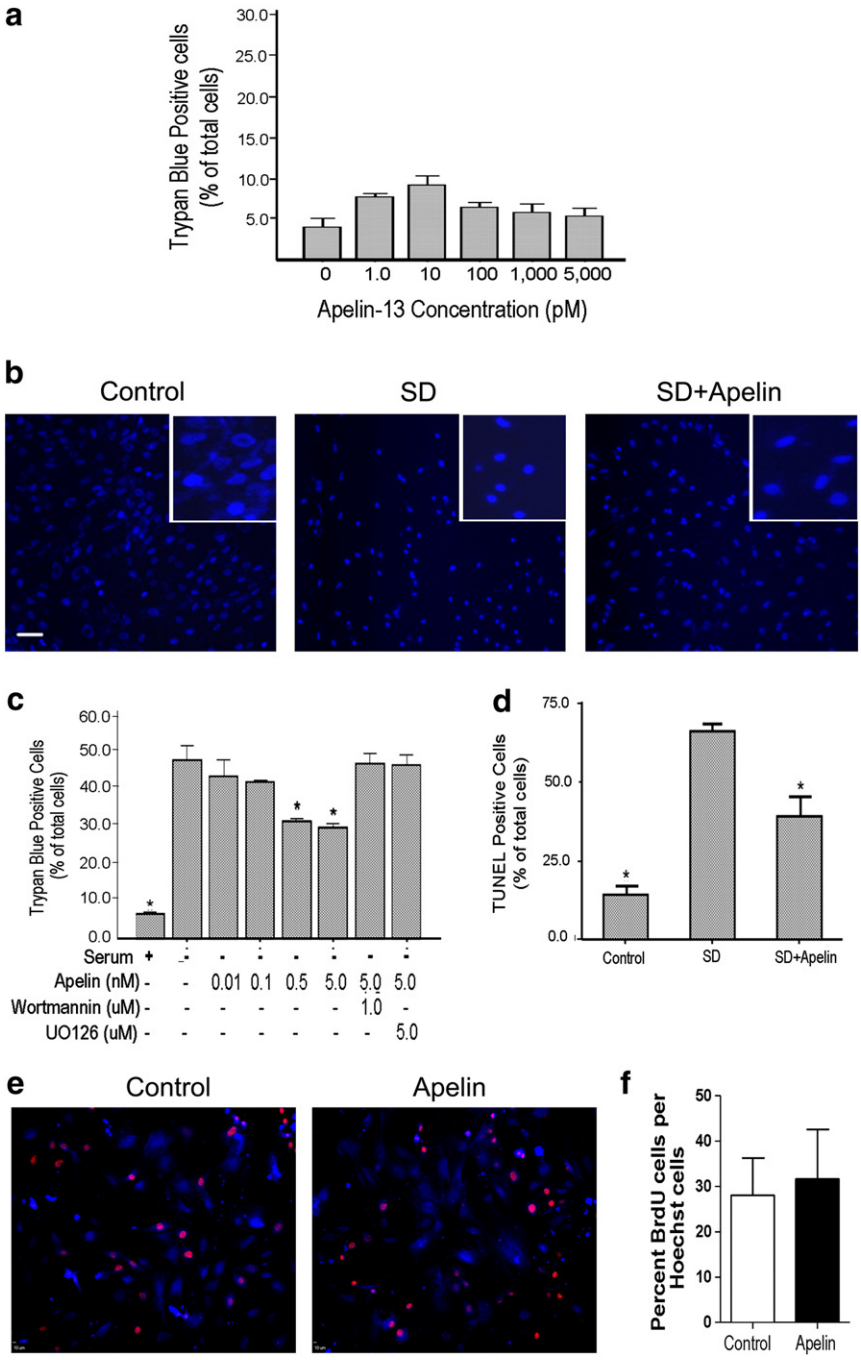


**Figure 2** *Effect of Apelin-13 on cell viability.* Apelin-13 was added into the culture media alone or co-applied with SD in order to test its effect on cell viability of BMSCs. a. Trypan blue assessment indicated that apelin-13 alone was not toxic to cultured BMSCs. Apelin-13 at 10 pM showed a trend of increasing the basal cell death, this phenomenon, however, was not seen with other concentrations of apelin-13. We conclude that this insignificant trend was likely due to the variation of cell culture conditions. b. Hoechst 33342 nuclear staining examined morphological changes of BMSC nuclei. SD treatment (36 h) caused marked cell shrinkage and nuclear condensation (inset images), both are typical apoptotic morphology. Co-applied apelin-13 (5 nM) noticeably blocked the cell shrinkage and nuclei condensation. c. Quantified data of trypan blue staining. The percentage of trypan blue positive cells vs. total cells was calculated and shown in the bar graph. SD caused about 40–50% cell death, which was decreased by co-applied apelin-13 in a concentration-dependent manner. The ERK1/2 blocker wortmannin (1 μM) and PI3K blocker UO126 (5 μM) reversed the apelin-13 effect, suggesting a mediator role of these signaling pathways (see Fig. 6 and corresponding text for more information). d. TUNEL staining was used to further evaluate SD-induced cell death and the protective effect of apelin-13, both showed similar results as seen in trypan blue experiments. e. Fluorescent imaging of BrdU (red) and Hoechst 33342 (blue) positive BMSCs. Cells were exposed to apelin-13 (5 nM) for 24 h and BrdU was added during the last 8 h to label proliferating cells. f. Summarized data of the ratio of BrdU-positive cells in control and apelin-13 treated cultures. $N \geq 3$ in each group. Mean ± SEM, $^{*}P < 0.05$ vs. SD.

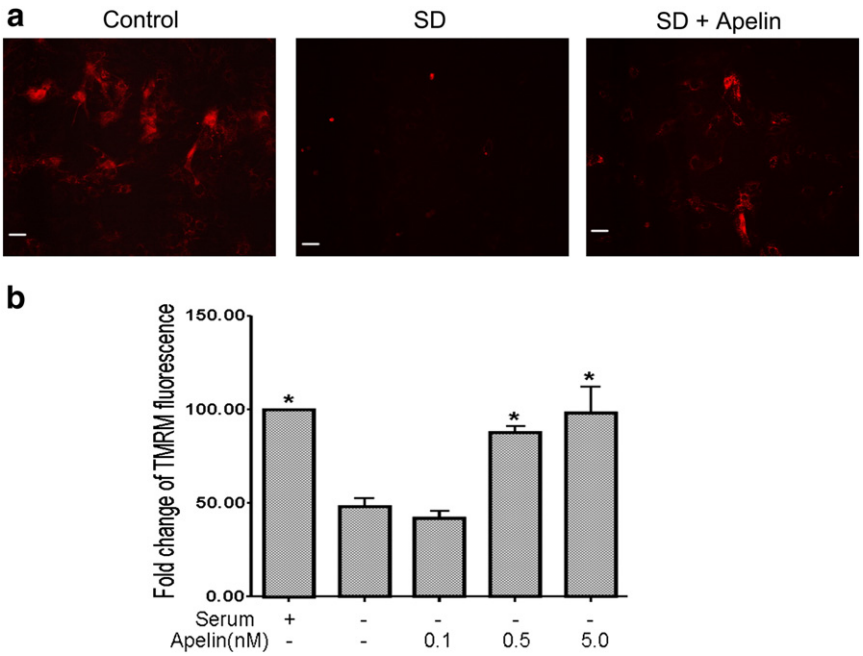


**Figure 3** *Effect of apelin-13 on the mitochondrial membrane potential*. The mitochondrial membrane potential was measured using TMRM fluorescence imaging in BMSCs. a. Control cells showed strong TMRM fluorescence indicative of normal membrane potential. After 12 h exposure to SD insult TMRM fluorescence decreased due to depolarization of the mitochondria. Apelin-13 (5 nM) added into the serum free media retained the mitochondrial membrane potential. b. Quantified data showing the protective effect of apelin-13 on the mitochondrial membrane potential. TMRM fluorescence decreased by 50% 12 h after SD while apelin-13 at 0.5 nM and 5 nM significantly reversed the loss of TMRM fluorescence. N = 3 independent assays per group; mean ± SEM, $^*P<0.05$ vs. SD group.

tissue cultures to evaluate ROS production reflected in excited red fluorescence in the nucleus. DHE fluorescent imaging was performed to detect ROS generation in BMSCs under different conditions. After 12 h of SD insult, DHE fluorescent-positive cells reached 38.5 ± 0.8% of total cells. This number of cells decreased to 26.0 ± 0.6% by 0.5 nM apelin-13 and 22.4 ± 2.3% by 5 nM apelin-13, respectively (Fig. 5).

### Roles of the MAPK/ERK1/2 and PI3K/Akt pathways in mediating apelin-13 effects

The MAPK/ERK and PI3K/Akt signaling pathways mediate the protective effects of apelin/APJ system in myocardial cells and neuronal cells (Zeng et al., 2009, 2010). We therefore investigated whether these pathways were involved in the anti-apoptotic effects of apelin-13 in BMSCs. Western blot analysis showed high levels of phospho-ERK1/2 in controls and low levels in SD treated cells (Fig. 6). Apelin-13 increased ERK1/2 phosphorylation in a concentration-dependent manner (Fig. 6a). To implicate ERK1/2 in apelin-induced protection against SD, BMSCs were treated with the specific blocker UO126 to inhibit this pathway. Analysis by trypan blue and Hoechst staining showed that UO126 (5 μM) attenuated the anti-apoptotic effect of apelin-13 (Fig. 2c). In parallel with its effect on phosphorylation of ERK1/2, apelin-13 caused a significant increase in Akt phosphorylation (Fig. 6b). Administration of the potent PI3K inhibitor, wortmannin (1 μM), markedly blocked the anti-apoptotic actions of apelin-13 (Fig. 2c).

## Discussion

Although BMSCs transplantation therapy has attracted considerable interest in recent years for repairing ischemia-damaged tissues in the heart and brain, its therapeutic exploitation has been limited by the fact that most of the transplanted BMSCs do not survive, presumably die from apoptosis due to insults from the ischemic environment. The present investigation demonstrates that apelin-13 can protect BMSCs from apoptotic cell death. We revealed that apelin-13 acts on retaining the mitochondrial membrane potential, preventing cytochrome c release from mitochondria, reducing the production of reactive oxygen species, and maintaining phosphorylation levels of ERK1/2 and Akt signaling pathways. Our observations suggest that apelin-13 may be explored as a supplemental strategy to improve the survival of BMSCs in transplantation therapy.

As an endogenous peptide, apelin has been shown to be protective against multiple insults in cardiomyocytes and neuronal cells (Simpkin et al., 2007; Zeng et al., 2009, 2010). Its effect on bone marrow stem cells has not been studied prior to this investigation. We demonstrated that BMSCs express the APJ receptor that is essential for the apelin action. This is consistent with a very recent report showing that the apelin-APJ pathway exists in BMSC-derived cardiomyogenic cells (Gao et al., 2010). The physiological function of endogenous apelin and APJ receptor in BMSCs is not clear. In the above report, the authors suggest that the expression of apelin-APJ pathway during differentiation of BMSCs into cardiomyogenic cells may regulate myocardial regeneration and functional recovery after BMSC

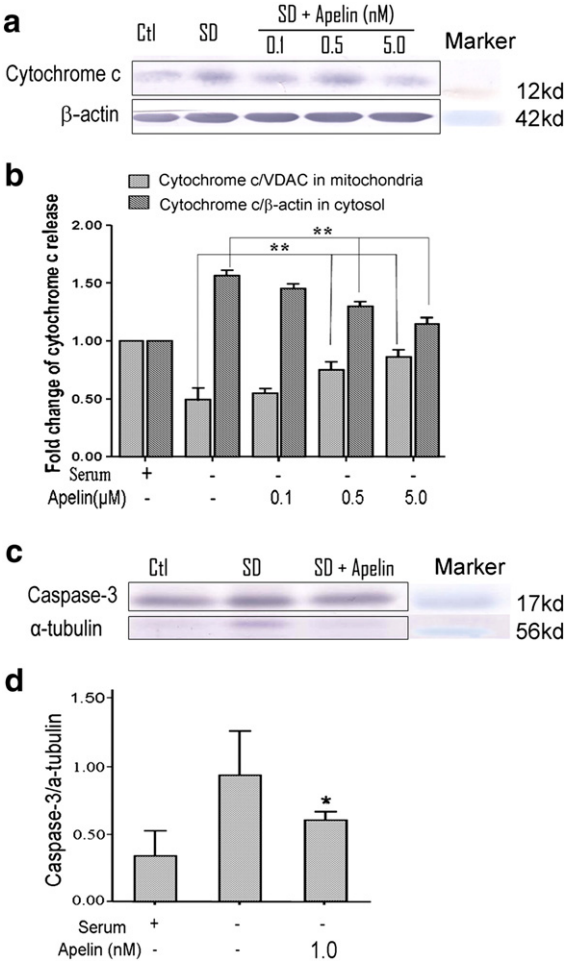


**Figure 4** *Effect of apelin-13 on cytochrome c release and caspase-3 activation.* Cytochrome c release and caspase-3 activation was tested 30 h after SD using Western blotting. a. Western blotting results of cytochrome c content in the cytosolic fraction of the cells. The cytochrome c level was high in SD treated cells. Apelin-13 showed inhibitory effect on the cytochrome c increase, especially at 5 nM concentration. b. Summary of normalized values of cytochrome c levels in the mitochondrial and cytosolic fractions of BMSCs. SD alone caused reduction of cytochrome c in the mitochondria accompanied by a corresponding increase in the cytoplasm. Apelin-13 reversed these apoptotic changes in a concentration-dependent manner. c. Caspase-3 activation was measured in cell lysates form different groups of cells. d. Quantified data of experiments in c. There was an increase in caspase-3 activity in SD treated BMSCs, Apelin-13 (1 nM) showed a significant effect of blocking this caspase-3 activation. Mean ± SEM. n = 3 assays per group. *$P<0.05$ vs SD group.

transplantation. Our work endorses the idea that apelin is also an important survival factor for BMSCs.

Apelin-13 showed a dose-dependent effect of antagonizing apoptosis in BMSCs. Multiple criteria was applied to identify the apoptotic nature of BMSC injury and the apelin-13 effect following serum deprivation (SD). The SD insult has its limitation; it does not mimic all aspects of an ischemic attack. However, this in vitro cell death model has the advantage of inducing typical "pure" apoptotic injury in neuronal and stem cell cultures, characterized by classical apoptotic changes in cell morphology and biological/biochemical assays (Yu et al., 1997; Valable et al., 2003). On the other hand, many in vitro and in vivo insults, such as hypoxia in vitro and ischemia in vivo, trigger mixed cell death composed of both necrosis and apoptosis (Xiao et al., 2002; Wei et al., 2004; Maurer et al., 1999). Therefore, SD is useful for understanding the cellular mechanism of the protective effect of apelin-13. We showed that apelin-13 effectively prevented SD-induced morphological alterations of cell shrinkage and nuclei condensation/fragmentation. Apelin-13 largely blocked several key apoptotic steps in the mitochondria-dependent apoptosis cascade. Cytochrome c is found in the mitochondria and released into the cytoplasm after mitochondrial membrane depolarization, leading to the formation of apoptosome, activation of caspase-3 and apoptosis (Kim et al., 2005). In our experiments, DHE imaging for ROS production revealed that SD-induced apoptosis was accompanied with increased ROS production while apelin-13 dose-dependently decreased DHE positive cells. This event is likely associated with SD-induced mitochondrial damage and the underlying apelin protective effect. TMRM imaging was used to reveal mitochondrial potential changes. Consistent with its effect on ROS production, apelin-13 effectively prevented this mitochondrial depolarization and consequent events. Whether apelin-13 could affect the apoptosis extrinsic pathway that is not mitochondria-dependent remains to be tested. In our previous investigation, we showed that apelin-13 not only blocked apoptosis in neuronal cells, it also prevented NMDA receptor-mediated excitotoxicity (Zeng et al., 2010). This apelin-13 action, however, was not tested in the present study on non-differentiated BMSCs because of the expected absence of glutamate receptors in these cells. Since BMSCs can differentiate into neuronal cells and this differentiation may be a useful mechanism for regeneration of CNS tissues, it may be necessary to understand this protective mechanism in BMSC-derived neurons in a future investigation. Different from the serum deprivation experiment, we did not detect protective effect of apelin-13 against OGD-induced cell death. This is likely due to the fact that continuous exposures to OGD trigger mainly necrotic but not apoptotic cell death (Koh et al., 1995) and additionally implies that, for BMSCs, apelin's protective effect was mainly from its anti-apoptotic action which is the focus of this investigation and likely to be a significant component of ischemic pathology. Supporting the idea, previous work from our and other's groups has demonstrated protective effects of apelin-13 against ischemic damage in animal studies (Zeng et al., 2009, 2010; Tao et al., 2011).

One of the major transduction pathways for apelin signal depends on the interaction with a $G_i$-protein coupled to the APJ receptor, independently of Ras protein; although dependent on Protein Kinase C (PKC) (Masri et al., 2005). In addition to the adenyl cyclase inhibition pathway, apelin activates ERK pathways through a PTX (pertussis toxin) sensitive $G_{\alpha i}$ protein, in a PKC-dependent process (Masri et al., 2005). Endothelial cell proliferation control is activated by apelin through two mechanisms: one is ERK-dependent and the other is PI3K-dependent (Masri et al., 2004). Some of these events may be conducive to enhance cell survival. Our current data demonstrated that apelin/APJ exerts its anti-apoptotic effects in BMSCs through ERK and Akt pathways. We showed that inhibition of PI3K with the specific blocker wortmannin or blocking

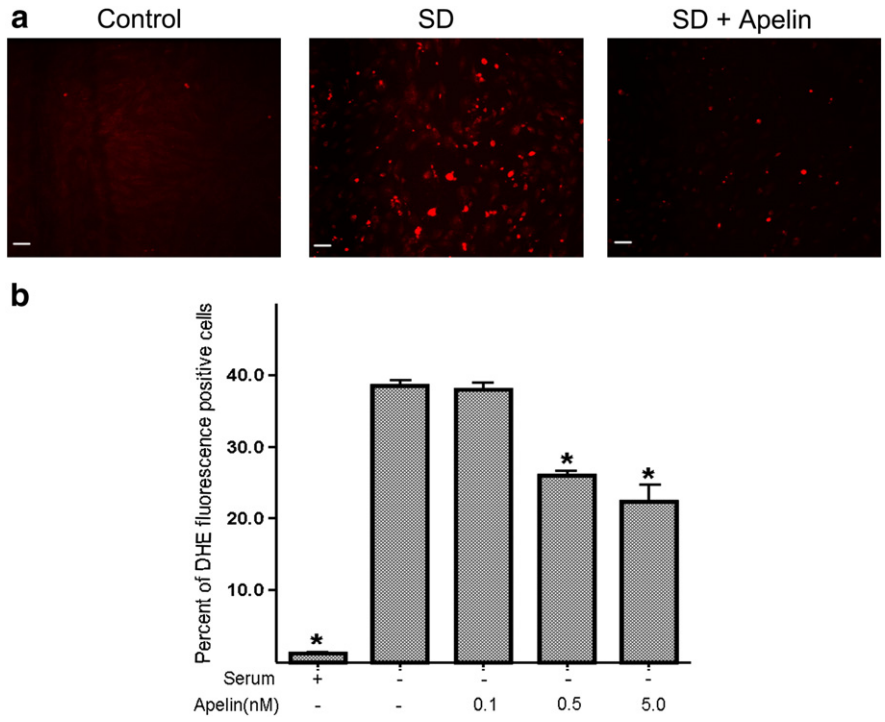


**Figure 5** *Effect of apelin-13 on reactive oxygen species production of apoptotic BMSCs.* Detection of ROS production in rat BMSCs using DHE fluorescence imaging. Cells were incubated with DHE for 5 min following 12 h SD treatment. Fluorescence was captured then quantitated for the total cells and DHE positive cells which displayed red fluorescence nuclear. a. DHE images showing the fluorescent images of control, SD-treated and SD plus apelin-13 (5 nM) cells. The increase fluorescent intensity in SD-treated cells indicted increased ROS production. b. Summary of experiments with different concentrations of apelin-13. Serum deprivation increased ROS generation while apelin-13 concentration-dependently decreased its production. Bars show the average percent of DHE fluorescent positive cells to total cells. N = 3 assays; mean ± SEM, *$P<0.05$.

ERK with UO126 effectively reversed the protective effects of apelin-13. These observations are consistent with previous investigations on cardiomyocytes and neuronal cells from our and other groups (Zeng et al., 2009, 2010; Masri et al., 2004; O'Donnell et al., 2007). In our experiments, apelin-13 did not stimulate proliferation of BMSCs. The regulatory mechanism for proliferation of BMSCs is not well defined. Our data implies that proliferation of BMSCs is not under direct regulation of apelin/APJ signaling.

In summary, we have presented novel data showing protective effects of apelin-13 against apoptosis in BMSCs. Apelin-13 effectively prevents several mitochondria associated apoptotic events and helps to regulate phosphorylation of the MAPK/ERK1/2 and PI3K/Akt pathways. It is feasible that apelin-13 conjugated with the APJ receptor can exert its pro-survival actions on BMSCs after transplantation. If so, apelin-13 may be applied to promote cell survival and therapeutic potential of stem cell therapy for ischemia related disorders such as heart ischemia and ischemic stroke.

## Materials and methods

### Rat BMSC cultures

BMSCs were isolated from Wistar rats as previously described (Hu et al., 2008). In brief, BMSCs were obtained from the femoral and tibial bones of rats. Cells were flushed from the femurs and tibias of rats using a 25-guage needle. Mononuclear cells were suspended in Dulbecco's modified Eagle's medium supplemented with 10% fetal bovine serum and plated in flasks. Cultures were maintained at 37 °C in a humidified atmosphere containing 5% carbon dioxide. After 24 h, non-adherent cells were discarded, and adherent cells were washed three times with phosphate-buffered saline solution (PBS). Fresh complete medium was added and replaced every 4 days. Each primary culture was subcultured 1:2 when BMSCs grew to 80% confluency.

### Bone marrow mesenchymal stem cell characterization

All cells used in assays were of passage 3 to 5. By the third passage, a homogenous population of fibroblast-like cells was obtained. To prevent hematopoietic cell contamination, which might be present in earlier passages, or the presence of senescent or differentiating BMSC in later passages, we used cells between passages three and five throughout the study. BMSCs used in our investigation have been fully characterized according to cell surface markers and multipotent differentiation assays; these data were reported in previous papers (Hu et al., 2008; Hu et al., n.a.). Briefly, flow cytometric analysis confirmed that these cells expressed CD73, CD90 and CD105 surface markers, but were CD34 and CD45 negative (Hu et al., 2008). The lack of expression of CD34

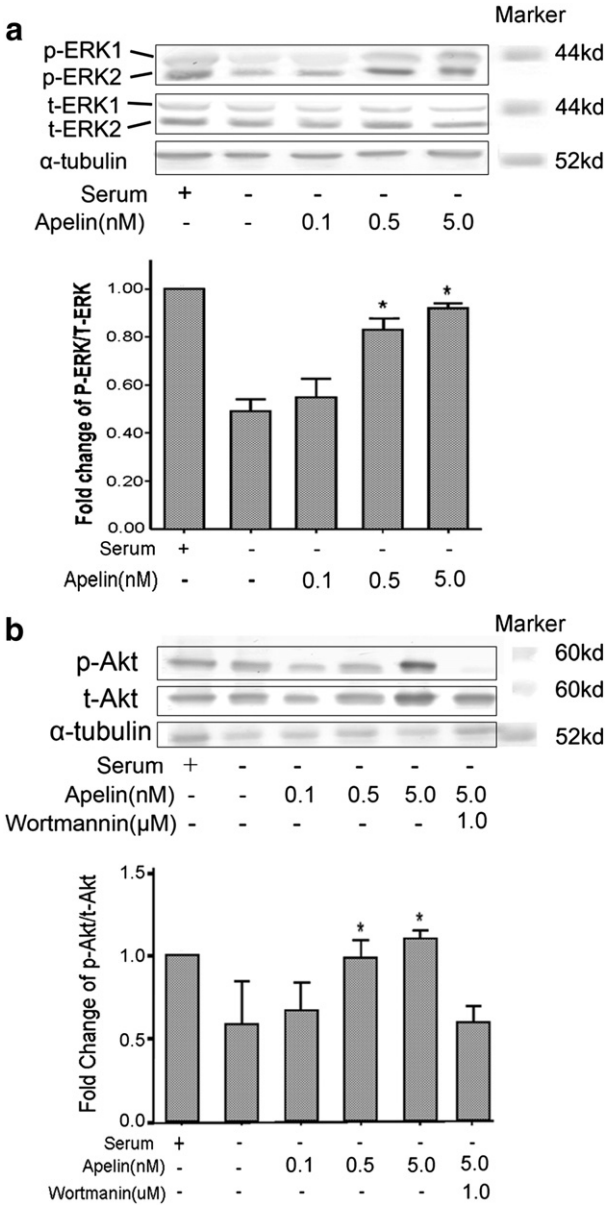


**Figure 6** *Effect of apelin-13 on ERK1/2 and Akt signaling pathways*. Western blotting was performed to assess protein levels of ERK1/2 and Akt in BMSCs after 6 h treatment with SD and the effect of co-applied apelin-13. a. The phosphor-ERK1/2 (p-ERK) and total ERK 1/2 (t-ERK) levels in BMSCs undergoing apoptosis and in the presence of different concentrations of apelin-13 (0.1 to 5.0 nM). The bar graph summarizes the densitometry of Western blotting, showing a reduction in the ratio of p-ERK/t-ERK in SD only cells and a concentration-dependent reverse of this ratio by apelin-13. b. Western blotting of phosphor-Akt (p-Akt) and total Akt (t-Akt) normalized to α-tubulin in BMSCs subjected to different treatments. Wortmannin was added to block PI3K that is upstream of Akt signaling. The bar graph of densitometry measurement shows reduction of p-Akt/t-Akt ratio (each level was normalized to α-tubulin), while apelin-13 at 0.5 and 5 nM prevented the p-Akt reduction. The apelin-13 effect was blocked by Wortmannin. N = 3 assays in each group; mean ± SEM; $^*P<0.05$ vs. SD group.

and CD45 confirmed that the cell population was depleted of hematopoietic stem cells. We have tested the multipotency of these cells as suggested by Dominici et al. (2006). The differentiation potential of these cells for becoming osteocyte and adipogenic cell phenotypes was confirmed (Hu et al., n.a.). The surface markers and multipotency property of these cells were thus highly consistent with the characteristics of bone marrow mesenchymal cells (Dominici et al., 2006).

## Detection of APJ expression on BMSCs

To confirm that APJ was expressed in our BMSCs, we used RT-PCR, immunofluorescent staining, and Western blot to detect APJ expression in these cells. Briefly, total RNA was extracted from cultured BMSCs using the RNAeasy Mini prep kit (Qiagen Inc, Valencia, CA) according to the manufacturer's instructions. Promega reverse transcription system (Promega Corp., Madison, WI) was used to reverse transcribe total RNA (2 μg) into first strand cDNA with Oligo (dT)18 primer. After that, the total length of rat APJ primers forward 5′ ATGGAAGATGATGGTTACA 3′ and reverse 5′ GTCCACAAGGGTTTCTTGGC 3′ were used to amplify rat APJ. Taq4 polymerase was used with an initial denaturation at 94 °C for 5 min followed by 30 cycles of 95 °C for 45 s, 54 °C for 45 s, 72 °C for 1.5 min and a final extension step at 72 °C for 10 min. PCR products were ran and imaged on an 1.0% agarose gels stained with ethidium bromide. Expected fragment sizes of 1121 bp, for a plasmid template from PcDNA3.1+/APJ was used as a positive control. Human embryonic kidney HEK293 cells were used as a negative control for the primers.

For Immunofluorescence staining, cultured BMSCs were fixed with 100% methanol for 5 min, and subjected to permeabilization with 0.2% triton X-100. After blocking with 1% fish gel in PBS for 1 h at room temperature, a primary antibody was added and incubated at 4 °C overnight. The primary antibody anti-APJ (rabbit anti-APJ polyclonal antibody; APJR-1H-300) was purchased from Santa Cruz (Santa Cruz Biotechnology, Inc., Santa Cruz, CA) and the anti-CD90 antibody was purchased from Abcam (Cambridge, MA). The antibodies were diluted to 2 μg/ml in PBS. The next day, the dishes were balanced at room temperature for 1 h and washed with PBS three times, then incubated for 2 h at room temperature in PBS containing secondary antibody: donkey anti-Rabbit IgG polyclonal antibody (488 conjugate, 500 μg; Chemicon/Millpore Corporation, Billerica, MA) diluted to 1 μg/ml. After washing with PBS three times Hoechst 33342 (Molecular Probes, Carlsbad, CA) at 1:20,000 in PBS was added and incubated for 5 min followed by three PBS washes. Coverslips were mounted on the bottom of the dishes in VECTASHIELD Mounting Medium (10 ml; Vector Laboratories, Inc., Burlingame, CA). Micrographs were captured on an Olympus IX61 microscope at 20× magnification.

To detect APJ expression in BMSCs, 40 μg of protein harvested from cultured BMSCs was subjected to sodium dodecyl sulfate–polyacrylamide gel electrophoresis, the primary antibody was the same antibody used in staining, the secondary antibody used was alkaline phosphatase — conjugated (Cell Signaling Technology, Danvers, MA) at a 1:2000 dilution, and the membranes were developed by the addition of BCIP/NBT solution (Sigma-Aldrich, St. Louis, MO).

### Apelin-13 toxicity assay on rat BMSCs

We tested potential toxicity of apelin at different concentrations on cultured rat BMSCs. BMSCs were incubated with apelin-13 (synthesized Apelin-13 trifluoroacetate salt, $\geq$95% purity; Sigma-Aldrich) in culture medium for 36 h. According to the material information provided by the manufacturer, the compound does not contain bacteria endotoxin or other hazardous substance. Trypan blue was added into the medium then incubated at 37 °C for 15 min before phase contrast graphs were taken by a microscope and trypan blue positive cells were counted. Five fields were randomly selected for every dish and at least three dishes were counted for every concentration.

### Serum deprivation-induced cell death of rat BMSCs

BMSCs were exposed to control, serum-free medium, and serum-free plus apelin-13 media for 36 h. Cell morphology was photographed using a phase-contrast microscope (Nikon Corp. New York, NY). Nuclear condensation and fragmentation was assessed using chromatin dye Hoechst 33342 as previously described. Apoptotic cells were characterized by morphological alteration such as condensed nuclei and cell shrinkage. Cell death was analyzed using Trypan blue staining and Terminal deoxynucleotidyltransferase-mediated DUTP-biotin nick end labeling (TUNEL) staining. A TUNEL staining kit, DeadEnd™ Fluorometric TUNEL System (Promega Corp.) was used for TUNEL staining according to the manufacturer's instruction. Briefly, cells were fixed by 10% formalin, cell permeabilization was done with 0.2% Triton X-100, equilibrated with equilibration Buffer for 10 min and incubated in rTdT Incubation Buffer for 60 min at 37 °C, then in 2× SSC for 15 min at room temperature and incubated with Hoechst 33342 (1:20,000) for 5 min. The dish was mounted in VECTASHIELD Mounting Medium (Vector Laboratories, Inc.).

Cell counting was performed in five non-overlapping fields captured on an Olympus IX61 microscope at 20× magnification. The percentage of Trypan blue positive and TUNEL positive cells vs. total cells was counted and calculated. At least 1000 BMSCs were counted for every dish and averaged, at least three dishes were counted for every group.

### Oxygen-glucose deprivation induced BMSC cell death

Oxygen and glucose deprivation (OGD) was employed to induce cell death in BMSC cultures. BMSC cultures of passages 3 to 5 were plated in 96 well plates and allowed to attach overnight in standard culture media. To initiate OGD condition, cells were washed in PBS twice and then incubated in a physiological buffer solution lacking glucose (120 mM NaCl, 25 mM Tris–HCl, 5.4 mM KCl, 1.8 mM $CaCl_2$, pH to 7.4 with NaOH). Cells were incubated in a calibrated hypoxia chamber perfused with 5% $CO_2$ and balanced Nitrogen for a final ambient oxygen level of 0.2%. Oxygen level was established, maintained and monitored by the ProOx 360 sensor (Biospherix, NY). After specified duration of OGD exposure, cells were "reperfused" by return to the normal 5% $CO_2$ incubator and normal oxygenated culture media. To test the effect of Apelin-13 on OGD-induced cell death, Apelin-13 was co-applied during the OGD. Apelin-13 was also re-applied upon reperfusion. Cell viability assay was initiated by adding MTT (0.5 mg/ml; Thiazolyl Blue Tetrazolium Bromide) 24 h after the onset of OGD followed by solubilization (20% SDS in 0.1 N HCl) overnight before measuring the MTT reaction in a plate reader. Cell viability was normalized to control non-OGD treated parallel cultures.

### Proliferation assay of BMSCs

BMSC cells of P2–P5 were plated in 35-mm Petri dishes, 5 nM apelin was added to treat cells for 24 h. BrdU (10 Um) was added during the last 8 h to label proliferating cells. After BrdU incorporation, cells were fixed by 4% paraformaldehyde for 15 min and followed by BrdU immunostaining. Briefly, cells were treated with 2 N HCl for 1 h, followed by 45 min in 0.2% Triton-X 100. After 1% fish gel blocking for 1 h, rat anti-BrdU antibody (1:400; Abcam, Cambridge, UK) was applied overnight. Cells were incubated with secondary antibody Cy3-conjugated anti-rat IgG (1:400; Invitrogen) for 1 h. Staining was visualized by fluorescent microscopy (BX61; Olympus, Tokyo, Japan). Numbers of BrdU positive cells were calculated by counting 6 random fields in each dish with three dishes per group. The results are presented as percentage of BrdU-positive cells per total cells (Hoechst 33342 staining).

### Analysis of mitochondrial membrane potential and cyochrome c release

The mitochondrial membrane potential dye, tetramethylrhodamine methyl ester (TMRM; Invitrogen) was loaded for 30 min at 37 °C in the dark, the cells were washed in fresh media, and treated with SD with or without apelin-13 for 12 h. TMRM was excited at 543 nM, 25% of the dye was present in the buffer during the entire course of the experiment. TMRM fluorescence was then measured under a fluorescence microscope. The quantification of the results was taken with the Image J software (NIH, Maryland, MD).

For the analysis of cytochrome c release from mitochondria, mitochondrial and cytosol proteins were extracted with the Mitochondria Isolation kit (Pierce, Rockford, IL) according to the manufacturer's protocols. Briefly, cells were incubated with 1.0 ml Cytosol Extraction Buffer Mix for 10 min, and homogenized using an ice-cold Dounce tissue grinder. The homogenates were centrifuged at 700 g and then the supernatants were further centrifuged at 10,000 *g* for 30 min at 4 °C. The cytosolic supernatants were decanted and the pellets were resuspended in 0.1 ml mitochondrial extraction buffer mix. Both the mitochondrial and cytosolic fractions were subjected to standard Western blotting and probed with a mouse monoclonal anti-rat cytochrome c antibody.

### Measurement of intracellular reactive oxygen species (ROS)

ROS production was measured using the specific dye dihydroethidium (DHE; Molecular Probes) prepared in DMSO. The stock solutions were diluted in tissue culture media to

the desired concentrations. Cells were incubated with 5 μmol/l DHE. Briefly, after experimental treatments, cells were incubated with 5 μmol/l DHE and 1:10,000 Hoechst 33342 in culture media for 5 min at 37 °C in the dark, and then fluorescent images were taken to count the percentage of DHE positive nuclear cells. Three independent experiments were performed.

### Protein extraction and Western blot analysis

For analysis of cellular protein levels, cells were rinsed twice with ice-cold PBS and lysed in ice-cold lysis buffer (20 mM Tris at pH 7.5), 150 mM NaCl, 1 mM EDTA, 1 mM EGTA, 1% TritonX-100, 2.5 mM sodium pyrophosphate, 1 mM β-glycerol glycerolphosphate, 1 mM Na3VO4, 1 mM PMSF, and 10 μg/ml each of Leupeptin, Aprotinin, and Pepstatin) for 30 min. Cell lysates were centrifuged at 13,000 *g* for 10 min at 4 °C and the protein concentration was determined by the BCA assay. Equal amounts of protein was determined and loaded per lane. The protein samples were mixed with 5× SDS sample buffer, boiled for 5 min and separated on 6%–18% SDS-PAGE gels before transferring the proteins onto a PVDF membrane by humid transfer. After blocking in 5% BSA for 1 h, membranes were rinsed and incubated overnight at 4 °C with the appropriate diluted primary antibody in 5% BSA, 1× TBS, and 0.1% Tween-20 (TBS/T), with gentle shaking. Excess antibody was removed by washing the membrane in TBS/T and subsequently incubated for 1 h with AP-conjugated secondary antibody at room temperature. After further washing in TBS/T, bands were developed by the addition of BCIP/NBT solution (Sigma-Aldrich). The membrane was scanned and analyzed by densitometry using Adobe Photoshop (Adobe Systems Inc., San Jose, CA) and Image J. Signal intensities of phosphorylated proteins were normalized to α-tubulin.

### Statistical analysis

Data expressed as mean ± SEM. Differences among groups were tested by one-way ANOVA. Comparisons between two groups were evaluated using LSD (least significant difference) *t* test. A value of $p<0.05$ was considered as significantly different.

## Acknowledgments

This work was supported by NIH grants NS 045810 (LW), NS062097 (LW), NS 058710 (LW), NS057255 (SPY) and the American Heart Association Established Investigator Award (LW). It was also supported by the NIH grant NS055077 to the ENNCF (Emory Neurology-NINDS Core Facility).

## References

Azizi, S.A., Stokes, D., Augelli, B.J., DiGirolamo, C., Prockop, D.J., 1998. Engraftment and migration of human bone marrow stromal cells implanted in the brains of albino rats—similarities to astrocyte grafts. Proc. Natl. Acad. Sci. U. S. A. 95, 3908–3913.

Barry, F.P., Murphy, J.M., 2004. Mesenchymal stem cells: clinical applications and biological characterization. Int. J. Biochem. Cell Biol. 36, 568–584.

Behrens, M.I., Koh, J.Y., Muller, M.C., Choi, D.W., 1996. NADPH diaphorase-containing striatal or cortical neurons are resistant to apoptosis. Neurobiol. Dis. 3, 72–75.

Chang, S.H., Poser, S., Xia, Z., 2004. A novel role for serum response factor in neuronal survival. J. Neurosci. 24, 2277–2285.

Chauvier, D., Lecoeur, H., Langonne, A., Borgne-Sanchez, A., Mariani, J., Martinou, J.C., Rebouillat, D., Jacotot, E., 2005. Upstream control of apoptosis by caspase-2 in serum-deprived primary neurons. Apoptosis 10, 1243–1259.

Dominici, M., Le Blanc, K., Mueller, I., Slaper-Cortenbach, I., Marini, F., Krause, D., Deans, R., Keating, A., Prockop, D., Horwitz, E., 2006. Minimal criteria for defining multipotent mesenchymal stromal cells. The International Society for Cellular Therapy position statement. Cytotherapy 8, 315–317.

Falcao-Pires, I., Leite-Moreira, A.F., 2005. Apelin: a novel neurohumoral modulator of the cardiovascular system. Pathophysiologic importance and potential use as a therapeutic target. Rev. Port. Cardiol. 24, 1263–1276.

Gao, L.R., Zhang, N.K., Bai, J., Ding, Q.A., Wang, Z.G., Zhu, Z.M., Fei, Y.X., Yang, Y., Xu, R.Y., Chen, Y., 2010. The apelin-APJ pathway exists in cardiomyogenic cells- derived from mesenchymal stem cells in vitro and in vivo. Cell Transplant. 19, 949–958.

Geng, Y.J., 2003. Molecular mechanisms for cardiovascular stem cell apoptosis and growth in the hearts with atherosclerotic coronary disease and ischemic heart failure. Ann. N. Y. Acad. Sci. 1010, 687–697.

Hu, X., Yu, S.P., Fraser, J.L., Lu, Z., Ogle, M.E., Wang, J.A., Wei, L., 2008. Transplantation of hypoxia-preconditioned mesenchymal stem cells improves infarcted heart function via enhanced survival of implanted cells and angiogenesis. J. Thorac. Cardiovasc. Surg. 135, 799–808.

Hu, X., Wei, L., Taylor, T.M., Wei, J., Zhou, X., Wang, J.A., Yu, S.P., 2011. Hypoxic preconditioning enhances bone marrow mesenchymal stem cell migration via Kv2.1 channel and FAK activation. Am. J. Physiol. Cell Physiol. 301, C362–372.

Kim, H.E., Du, F., Fang, M., Wang, X., 2005. Formation of apoptosome is initiated by cytochrome c-induced dATP hydrolysis and subsequent nucleotide exchange on Apaf-1. Proc. Natl. Acad. Sci. U. S. A. 102, 17545–17550.

Kleinz, M.J., Davenport, A.P., 2005. Emerging roles of apelin in biology and medicine. Pharmacol. Ther. 107, 198–211.

Koh, J.Y., Gwag, B.J., Lobner, D., Choi, D.W., 1995. Potentiated necrosis of cultured cortical neurons by neurotrophins. Science 268, 573–575.

Lee, H.J., Tomioka, M., Takaki, Y., Masumoto, H., Saido, T.C., 2000. Molecular cloning and expression of aminopeptidase A isoforms from rat hippocampus. Biochim. Biophys. Acta 1493, 273–278.

Li, Y., Chen, J., Wang, L., Lu, M., Chopp, M., 2001. Treatment of stroke in rat with intracarotid administration of marrow stromal cells. Neurology 56, 1666–1672.

Masri, B., Morin, N., Cornu, M., Knibiehler, B., Audigier, Y., 2004. Apelin (65–77) activates p70 S6 kinase and is mitogenic for umbilical endothelial cells. FASEB J. 18, 1909–1911.

Masri, B., Knibiehler, B., Audigier, Y., 2005. Apelin signalling: a promising pathway from cloning to pharmacology. Cell. Signal. 17, 415–426.

Maurer, B.J., Metelitsa, L.S., Seeger, R.C., Cabot, M.C., Reynolds, C.P., 1999. Increase of ceramide and induction of mixed apoptosis/necrosis by N-(4-hydroxyphenyl)- retinamide in neuroblastoma cell lines. J. Natl. Cancer Inst. 91, 1138–1146.

O'Donnell, L.A., Agrawal, A., Sabnekar, P., Dichter, M.A., Lynch, D.R., Kolson, D.L., 2007. Apelin, an endogenous neuronal peptide, protects hippocampal neurons against excitotoxic injury. J. Neurochem. 102, 1905–1917.

O'Dowd, B.F., Heiber, M., Chan, A., Heng, H.H., Tsui, L.C., Kennedy, J.L., Shi, X., Petronis, A., George, S.R., Nguyen, T., 1993. A human gene that shows identity with the gene encoding the angiotensin receptor is located on chromosome 11. Gene 136, 355–360.

Pereira, R.F., Halford, K.W., O'Hara, M.D., Leeper, D.B., Sokolov, B.P., Pollard, M.D., Bagasra, O., Prockop, D.J., 1995. Cultured adherent cells from marrow can serve as long-lasting precursor cells for bone, cartilage, and lung in irradiated mice. Proc. Natl. Acad. Sci. U. S. A. 92, 4857–4861.

Simpkin, J.C., Yellon, D.M., Davidson, S.M., Lim, S.Y., Wynne, A.M., Smith, C.C., 2007. Apelin-13 and apelin-36 exhibit direct cardioprotective activity against ischemia-reperfusion injury. Basic Res. Cardiol. 102, 518–528.

Tang, S.Y., Xie, H., Yuan, L.Q., Luo, X.H., Huang, J., Cui, R.R., Zhou, H.D., Wu, X.P., Liao, E.Y., 2007. Apelin stimulates proliferation and suppresses apoptosis of mouse osteoblastic cell line MC3T3-E1 via JNK and PI3-K/Akt signaling pathways. Peptides 28, 708–718.

Tao, J., Zhu, W., Li, Y., Xin, P., Li, J., Liu, M., Redington, A.N., Wei, M., 2011. Apelin-13 protects the heart against ischemia-reperfusion injury through inhibition of ER-dependent apoptotic pathways in a time-dependent fashion. Am. J. Physiol. Heart Circ. Physiol. 301, H1471–H1486.

Tatemoto, K., Hosoya, M., Habata, Y., Fujii, R., Kakegawa, T., Zou, M.X., Kawamata, Y., Fukusumi, S., Hinuma, S., Kitada, C., Kurokawa, T., Onda, H., Fujino, M., 1998. Isolation and characterization of a novel endogenous peptide ligand for the human APJ receptor. Biochem. Biophys. Res. Commun. 251, 471–476.

Toma, C., Pittenger, M.F., Cahill, K.S., Byrne, B.J., Kessler, P.D., 2002. Human mesenchymal stem cells differentiate to a cardiomyocyte phenotype in the adult murine heart. Circulation 105, 93–98.

Tsubokawa, T., Yagi, K., Nakanishi, C., Zuka, M., Nohara, A., Ino, H., Fujino, N., Konno, T., Kawashiri, M.A., Ishibashi-Ueda, H., Nagaya, N., Yamagishi, M., 2010. Impact of anti-apoptotic and anti-oxidative effects of bone marrow mesenchymal stem cells with transient overexpression of heme oxygenase-1 on myocardial ischemia. Am. J. Physiol. Heart Circ. Physiol. 298, H1320–H1329.

Valable, S., Bellail, A., Lesne, S., Liot, G., Mackenzie, E.T., Vivien, D., Bernaudin, M., Petit, E., 2003. Angiopoietin-1-induced PI3-kinase activation prevents neuronal apoptosis. FASEB J. 17, 443–445.

Wei, L., Ying, D.J., Cui, L., Langsdorf, J., Yu, S.P., 2004. Necrosis, apoptosis and hybrid death in the cortex and thalamus after barrel cortex ischemia in rats. Brain Res. 1022, 54–61.

Xiao, A.Y., Wei, L., Xia, S., Rothman, S., Yu, S.P., 2002. Ionic mechanism of ouabain-induced concurrent apoptosis and necrosis in individual cultured cortical neurons. J. Neurosci. 22, 1350–1362.

Xie, H.Q., Yang, Z.M., Xin, J.P., 2000. Short tandem repeat loci examination after repair of coracoclavicular ligament injury by tissue engineered tendon. Zhongguo Xiu Fu Chong Jian Wai Ke Za Zhi 14, 237–240.

Yu, S.P., Yeh, C.H., Sensi, S.L., Gwag, B.J., Canzoniero, L.M., Farhangrazi, Z.S., Ying, H.S., Tian, M., Dugan, L.L., Choi, D.W., 1997. Mediation of neuronal apoptosis by enhancement of outward potassium current. Science 278, 114–117.

Zeng, X.J., Zhang, L.K., Wang, H.X., Lu, L.Q., Ma, L.Q., Tang, C.S., 2009. Apelin protects heart against ischemia/reperfusion injury in rat. Peptides 30, 1144–1152.

Zeng, X.J., Yu, S.P., Zhang, L., Wei, L., 2010. Neuroprotective effect of the endogenous neural peptide apelin in cultured mouse cortical neurons. Exp. Cell Res. 316, 1773–1783.

Zhang, M., Methot, D., Poppa, V., Fujio, Y., Walsh, K., Murry, C.E., 2001. Cardiomyocyte grafting for cardiac repair: graft cell death and anti-death strategies. J. Mol. Cell. Cardiol. 33, 907–921.

Zubko, R., Frishman, W., 2009. Stem cell therapy for the kidney? Am. J. Ther. 16, 247–256.